Nonlinear Dynamic Rupture in Sapphire

Dov Sherman and Ilan Be'ery
Department of Materials Engineering, Technion-Israel Institute of Technology, Haifa 32000, Israel
(Received 26 June 1997)

Thin, wide, strips like sapphire specimens were fractured under three point bending. The fracture surfaces of the specimens were investigated using nonlinear analysis. The crack profiles were analyzed using correlation dimension, false nearest neighbor, and null hypothesis surrogate data methods and found to be a spatial occurrence of a chaotic deterministic system with at least seven dimensions, in contrast to only one independent variable used in current analytical calculations. [S0031-9007(97)05036-9]

PACS numbers: 62.20.Mk, 05.45.+b, 46.30.Nz

Phenomenological observations in many classes of brittle materials have shown an almost universal route of instability as the unbalanced energy increases in cracked bodies that occur in the following sequence: mirror, mist hackle, and branching [1–3]. Fineberg *et al.* [4] have measured the crack velocity in polymethylmethacrylate (PMMA), and found velocity oscillations that coincide with the jagged structure of the fracture surface. Crack oscillations in sapphire were reported by Wiederhorn [5] when the K_I direction was parallel to (0001) and $(\bar{1}012)$ planes. No oscillations were detected on the $(10\bar{1}0)$ plane. Ball and Payne [6] have reported oscillation on some fracture planes of quartz crystals. These oscillations were not stable, but rather grew in amplitude until branching occurred. In a previous work we have shown that a crack in single crystal should have oscillations even for low unbalanced energy but with very low amplitude [7].

The nature of the equations of motion of a rapid crack is not well known yet. An analytical approach, based on continuum elastic theory [1] has led to a one-dimensional crack-tip equation of motion. Nonlinear analysis enables one to investigate a dynamical system near steady state and to determine the characteristics of the system by examining one or more variables as a function of time or other integration variable. This investigation is aimed at demonstrating that crack propagation in single crystal material, under the described loading, is a chaotic deterministic process rather than a random one, and should be described by a high order differential equation.

In this investigation, 0.5 mm thick 50×10 mm^2 rectangular sapphire slabs were tested. The surfaces of the slabs were parallel to the (0001) plane, the normal [0001] to these surfaces is shown in Fig. 1. The short axis of the specimen inclined with 12° to the $(10\bar{1}0)$ cleavage plane. The specimens were loaded under three point bending (3PB) until fracture occurs. Detailed analysis of the fracture mechanisms was given in previous work [7].

Fractured specimens were placed horizontally in a Bakelite cast to replicate the fracture surfaces, and then removed from the cast, revealing the replicated fracture surface. We chose to analyze the low frequency, high amplitude perturbations [7]. The Bakelite was polished to the depth of the desired section of the crack surface. The crack profile was photographed and the resulting skyline was scanned and converted to numerical data. The result of the sampling process was a "time" series of 7480 points, which correspond to 9 mm in length. The time series is denoted by $y(x)$ where x and y are both spatial coordinates, and $\bar{y} = 0$. Since the actual scale of the data is irrelevant for most of the discussion below, the values of the functions are given in pixels. Roughly, the trajectory of the crack profile can be described by a set of triangular sawtooth with angle of 150°, suggesting that the crack moves alternatively on $(10\bar{1}0)$ and $(11\bar{2}0)$ cleavage planes.

The numerical crack profile is shown in Fig. 2(a). This profile represents a physical length of 5 mm. The x axis represents the crack profile coordinate self-similar to the crack direction, while the y axis represents the coordinate normal to the crack path (note the different scales). Assuming that the velocity of the crack tip is terminal at this zone, one can look upon the x coordinate as the time coordinate and $f(x) = f(t)$ as a time series of an unknown dynamic system.

We confronted the experimentally obtained crack profile with a phase and sequence randomization of that profile, and with three other randomly generated profiles, to determine whether the crack trajectory is a random function or chaotic deterministic motion. The randomly generated profiles, with a fixed angle of 150° were constructed using the equation $y^2 + B\,\mathrm{rand}(0;1) > C$ [Fig. 2(b)], where B and C were adjusted to obtain a similar amplitude

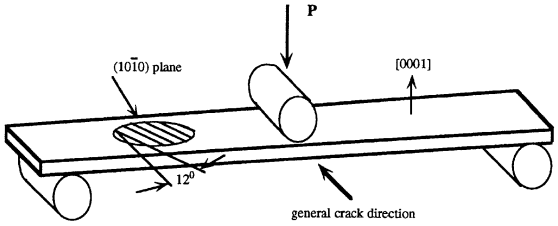

FIG. 1. Schematic presentation of the specimens' three point bend loading and relevant direction and plane.

 0031-9007/98/80(3)/540(4)$15.00

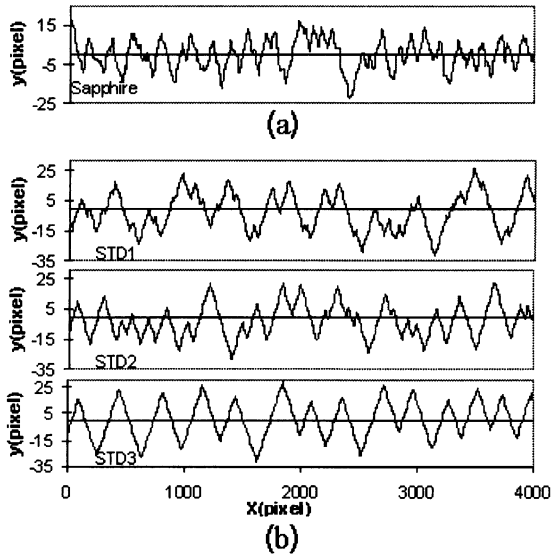

FIG. 2. The physical (a) and the randomly generated (b) crack profiles.

compared to the experimental profile, and STD1 to STD3 denoting, respectively, larger, similar, and smaller standard deviations of the distances between the peaks of the randomly generated profiles and that of the experimental profile.

The power spectrum is shown in Fig. 3. The power spectrum of the first and last 2000 data points, respectively, from the total 7480 data points is shown. The power spectrum does not have a dominant peak, but rather has components in a large domain of frequencies. The power spectrum changes only slightly from the beginning to the end of the sample. It is assumed that due to small change in the strain energy release rate during crack advance [7] the system changes adiabatically; i.e., the equations of motion change without violating equilibrium.

The most widely used phase space reconstruction is the time delay embedding [8,9]. In this method, an M dimensional vector $\mathbf{P}$ is reconstructed from the one-dimensional time series by sampling it at constant intervals: $\mathbf{P}(x;M) = \{y(x), y(x + x_0), y(x + 2x_0), \ldots, y(x + [M - 1]x_0)\}$. Given that M is large enough, and x_0 is properly selected, the plot of $\mathbf{P}(x;M)$ in an M dimensional space will reconstruct a manifold topologically equivalent to the system's attractor. An estimation of the embedding time delay, x_0, can be obtained by minimizing the mutual information [9–11], as shown in Fig. 4, indicating that the optimal embedding time delay for our data is 25 pixels. The time delay for the randomly generated profiles was chosen such that the mutual information equals the minimum of the experimental mutual information. An example of a reconstructed attractor of the experimental profile for $M = 2$ and $x_0 = 25$ is shown in Fig. 5. The crossing of many of the trajectories in this figure implies that it is a projection of a higher dimensional trajectory.

Three methods have been used to determine whether the time series are deterministic, and to calculate the optimal embedding dimension of the system. The methods are based on finding nearest neighbors (NN) in a reconstructed phase space. To minimize the influence of the change in the strain energy release rate, we limited the search space of the NN to a time window of 3000 pixels. We excluded the nearest 120 pixels out of the search space to cancel the effect of linear autocorrelation.

(I) Null hypothesis surrogate data (NHSD) [12].—The typical result of the NHSD test is a gradual decrease of Z (Z is the probability of rejecting the null hypothesis), with increasing dimension until a stabilization occurs when the optimal embedding dimension is reached. The situation for the examined profiles was different: Z dropped to its minimum at $M = 2$, and then climbed and stabilized at a higher value, Fig. 6. We postulate that this unusual result is due to the crystallographic angle characterizing our samples. NHSD test performed on the randomly generated profiles indicated a similar behavior. However, unlike the experimental profile, Z of the random data always climbed to a positive value at large dimensions. It is therefore concluded that the sapphire data is deterministic.

(II) False nearest neighbor (FNN) [9,10].—Denoting the Euclidean distance between a pair of NN by $R_M(n)$

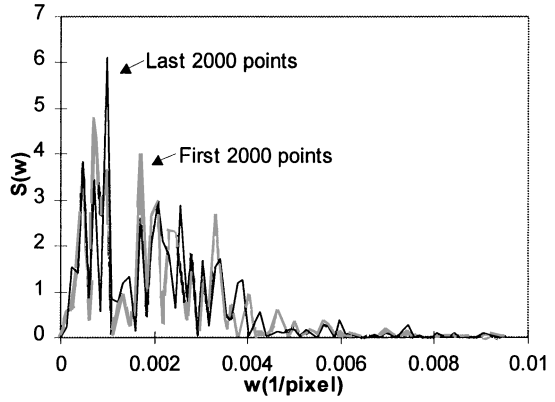

FIG. 3. The logarithm of the power spectrum of the crack profile.

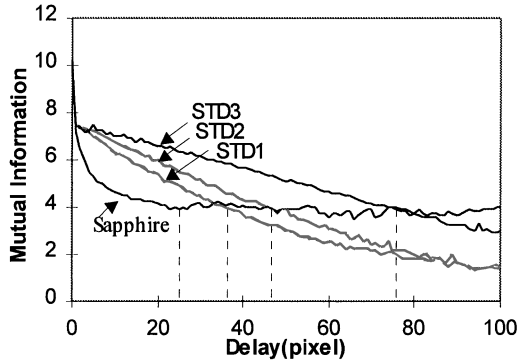

FIG. 4. The mutual information as a function of embedding interval for the experimental and the randomly generated profiles.

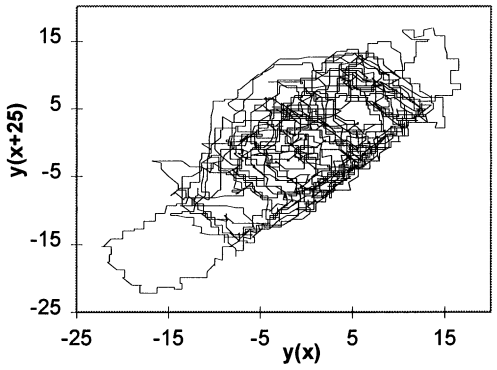

FIG. 5. Presentation of $y = f(x)$ and $y = f(x + x_0)$ with a phase shift of 25 pixels.

where M is the embedding dimension, and n the index of the pair, we can use the criterion for FNN: $\{[R_{M+1}^2(n) - R_M^2(n)]/R_M^2(n)\}^{1/2} > R_{\text{crit}}$ where R_{crit} is usually of the order of 10.

If the data set is small or noisy, many of the NN would not be close enough to allow further expansion, and the FNN test might give a false, underestimating dimension. To avoid this effect we used only those NN whose $R_M(n)$ is small compared to the STD^M (the standard deviation of the data sample in power of the embedding dimension).

We have compared the fraction of FNN as a function of the dimension for the original data, as well as for phase randomized (PR), sequence randomized (SR) (Fig. 7), and the randomly generated profile. The percentage of FNN of the randomized samples never decreases below 20% while it did drop to 0.4% for $M = 6$ and to zero for $M = 7$.

(III) Correlation dimension [10,11,13].—While the embedding dimension is essential for reconstructing the equations of motion of the system, it is the fractal dimension that helps us to understand the structure of the attractor manifold. The most commonly measured dimension is the correlation dimension denoted by D_2, which is smaller than the dimension of the dynamic system. To calculate the correlation dimension, one counts the number C of neighbors in a distance r from a given point and sums on all points: $C(r; M) = \lim_{N\to\infty}[N^{-2}\sum_{i=1}^{N}\sum_{j=1}^{N} H(r - |P_i - P_j|)]$ where H is the Heaviside step function and $||$ is the Euclidean M dimensional distance. The (physical) correlation dimension is defined as $D_2(M) = d\ln C(r)/d\ln(r)$, over some range in which this expression is relatively constant. As proposed by Grassberger and Procaccia [13], the correlation dimension is estimated for increasing embedding dimension. When the unfolding embedding dimension is reached, the correlation dimension reaches a steady value which is the correlation dimension of the attractor. Following Schmidt and Dünki [10] we used an improved version of the algorithm, including optimization of time delay, using decorrelation window when calculating $C(r)$, and a smart algorithm for the selection of the scaling region. The correlation dimension as a function of the embedding dimension for the test data and the two randomized data are shown in Fig. 8. For the randomized data the correlation dimension did not converge. We assumed asymptotic approach of $D_2(M)$ to its final value of the form: $D_2(M) = D_2^{\infty}(1 - e^{-bM})$, where D_2^{∞}

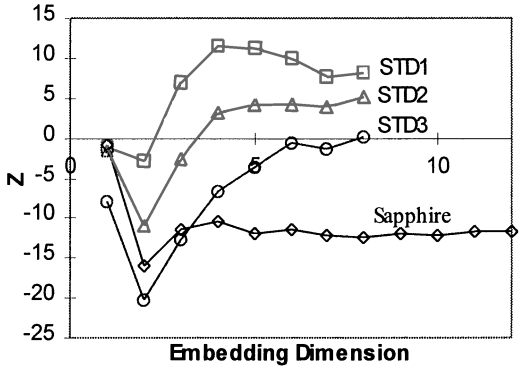

FIG. 6. Z value of the NHSD test as a function of the embedding dimension for the experimental and the randomly generated profiles.

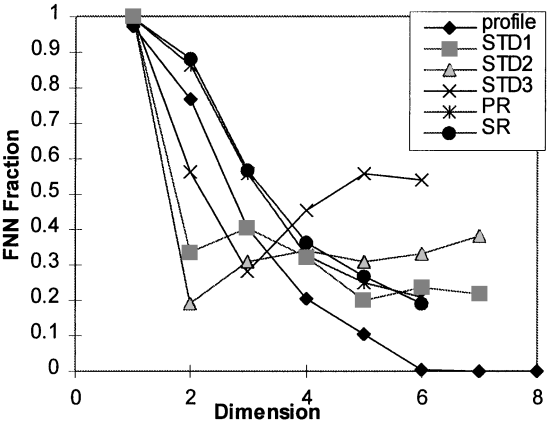

FIG. 7. The fraction of FNN as a function of the dimension for the experimental profile, phase randomized (PR) and sequence randomized (SR), and for the randomly generated profiles.

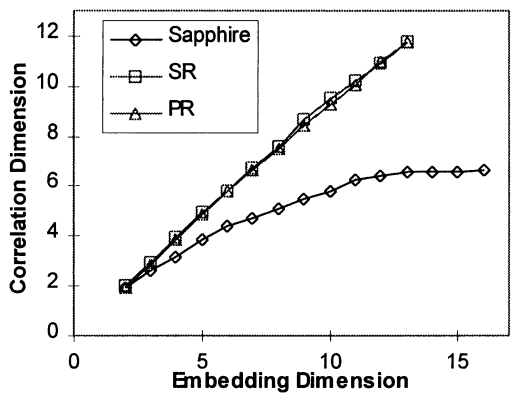

FIG. 8. The correlation dimension as a function of the embedding dimension (M) for the sapphire and its SR and PR.

is the correlation dimension of the unfolded attractor, and b is unknown. Using best fit of that form we obtained $D_2^{\infty} = 6.62 \pm 0.1$. We note that the maximum correlation dimension acceptable depends on the number of data points L as $D_2^{\max} \cong 2 \log_{10} L$ [14]. In the experimental profile, the value of $D_2^{\max}$ lies between 6.95 (for the 3000 pixel window) and 7.75 (for the whole data set). The dimension obtained is therefore close to the limiting value, but the scaling behavior of the correlation integral suggested it is at least close to the real value.

It is concluded from the above nonlinear analysis that the analyzed cracking process is chaotic deterministic in nature, and can be described by a set of differential equation of the order of 7 at least, in contrast to only one-dimensional analysis that has usually been done until now.

We gratefully acknowledge Irit Katriel for her help with the computer analysis of the dynamic chaotic system.

[1] L. B. Freund, *Dynamic Fracture Mechanics* (Cambridge University Press, Cambridge, 1990).
[2] B. Lawn, *Fracture of Brittle Solids*, Cambridge Solid State Science Series (Cambridge University Press, Cambridge, 1993), 2nd ed.
[3] R. W. Rice, in *Advances in Ceramics*, edited by V. D. Frechette and J. R. Varner (American Ceramic Society, Westerville, OH, 1986), Vol. 22, pp. 3–56.
[4] J. Fineberg *et al.*, Phys. Rev. B **45**, 5146 (1992).
[5] S. M. Wiederhorn, J. Am. Ceram. Soc. **52**, 485–491 (1969).
[6] A. Ball and B. W. Payne, J. Mater. Sci. **11**, 731–740 (1976).
[7] D. Sherman and I. Be'ery (to be published).
[8] N. H. Packard *et al.*, Phys. Rev. Lett. **45**, 712 (1980).
[9] A. H. Nayfeh and B. Balachandran, *Applied Nonlinear Dynamics*, Wiley Series in Nonlinear Science (J. Wiley & Sons, New York, 1995).
[10] G. B. Schmidt and R. M. Dünki, Physica (Amsterdam) **93D**, 165 (1996).
[11] H. D. I. Abarbanel, R. Brown, J. J. Sidorowich, and L. S. Tsimring, Rev. Mod. Phys. **65**, 1331 (1993).
[12] M. B. Kennel and S. Isabelle, Phys. Rev. A **46**, 3111 (1992).
[13] P. Grassberger and I. Procaccia, Phys. Rev. Lett. **50**, 346–349 (1983).
[14] J. P. Eckmann and D. Ruelle, Physica (Amsterdam) **56D**, 185 (1992).